PHYSICAL REVIEW D **93,** 055024 (2016)

Mass spectrum and Higgs profile in $B-L$ symmetric SSM

Cem Salih Ün[1,2,*] and Özer Özdal[3,†]

[1]*Center of Fundamental Physics, Zewail City of Science and Technology, 6 October City, 12588 Cairo, Egypt*
[2]*Department of Physics, Uludag University, TR16059 Bursa, Turkey*
[3]*Department of Physics, İzmir Institute of Technology, IZTECH, TR35430 İzmir, Turkey*

(Received 18 January 2016; published 17 March 2016)

We investigate the predictions on the mass spectrum and Higgs boson decays in the supersymmetric standard model extended by $U(1)_{B-L}$ symmetry (BLSSM). The model requires two singlet Higgs fields, which are responsible for the radiative breaking of $U(1)_{B-L}$ symmetry. It predicts degenerate right-handed neutrino masses (1.7–2.2 TeV) as well as the right-handed sneutrinos of mass $\lesssim$4 TeV. The presence of right-handed neutrinos and sneutrinos triggers the baryon and lepton number violation processes, until they decouple from the standard model particles. Besides, the model predicts rather heavy colored particles; $m_{\tilde{t}}$, $m_{\tilde{b}} \gtrsim 1.5$ TeV, while $m_{\tilde{\tau}} \gtrsim 100$ GeV and $m_{\tilde{\chi}_1^\pm} \gtrsim 600$ GeV. Even though the implications are similar to the minimal supersymmetric standard model, BLSSM can predict another Higgs boson lighter than 150 GeV. We find that the second Higgs boson can be degenerate with the lightest charge parity (CP)-even Higgs boson of mass about 125 GeV and contribute to the Higgs decay into two photons. In addition, it can provide an explanation for the excess in $h \to 4l$ at the mass scale $\sim$145 GeV.

DOI: 10.1103/PhysRevD.93.055024

I. INTRODUCTION

After the discovery of the Higgs boson of mass about 125–126 GeV by the ATLAS [1] and the CMS [2] experiments, analyses have confirmed that the standard model (SM) predictions are in a very good agreement with the observations. Despite the fact that the SM has been completed with the Higgs boson discovery, there is no doubt that the SM is not a fundamental theory, since it is problematic in the Higgs boson due to the gauge hierarchy problem [3] and the absolute stability of the Higgs potential [4]. However, experiments conducted at the Large Hadron Collider (LHC) have returned with no direct signal for new physics beyond the SM (BSM). In contrast, the experimental results almost overlap with the SM predictions. On the other hand, the Higgs boson may play a leading role in further analyses, since it provides strong hints for BSM. In addition to the observed mass of the Higgs boson, detailed analyses have revealed some anomalies in decay channels of the Higgs boson. While combination of all decay channels excludes the range $\sim 150 < m_h < 1000$ GeV [5], there is an excess in $h \to \gamma\gamma$ at $m_{\gamma\gamma} \approx 137$ GeV, in addition to that observed at $m_{\gamma\gamma} \approx 125$ GeV [6]. Similarly, $h \to 4l$ exhibits an excess at around $m_{4l} \approx 146$ GeV [7].

While one can count the SM Higgs boson for the observations at about 125 GeV, the anomalies at the higher scales can be considered as hints for the heavier SM-like Higgs bosons, which are not included in the SM. In this context, models with two or more Higgs bosons are worth studying in light of the anomalies mentioned above. Minimal supersymmetric extension of the SM (MSSM) is classified as a theory with two Higgs doublets and it is arguably one of the prime candidates for BSM, since it provides a resolution to the gauge hierarchy problem. The two Higgs doublets yield five physical Higgs boson states after electroweak symmetry breaking, and they may offer a number of different scenarios to explain the anomalies in decay modes of the Higgs bosons [8].

Even though it is possible to fit the low scale implications with the observed data in the MSSM framework, one can also consider the high scale origin, since the three gauge couplings of the SM nicely unify at the grand unification scale ($M_{\rm GUT} \approx 2 \times 10^{16}$ GeV). Stabilizing the Higgs boson mass at all the energy scales, one can connect $M_{\rm GUT}$ to the electroweak scale ($M_{\rm EW}$) through the renormalization group equations (RGEs). In such models, a large number of low scale MSSM parameters can be calculated through RGEs with a few free parameters defined at $M_{\rm GUT}$. Although MSSM is compatible with the current experimental results, the Higgs boson results bring severe constraints on the sparticle spectrum. As is well known, the tree-level Higgs boson mass prediction is inconsistently low in the MSSM, and hence, one needs to utilize the loop corrections in order to realize the observed Higgs boson mass. Since the first two families have negligible Yukawa couplings to the Higgs boson, the third family provides the main source for such contributions. The sbottom and stau contributions exhibit $\tan\beta$ enhancement, and they can easily destabilize the Higgs potential; hence, their contributions are strongly constrained by the vacuum stability which allows only minor contributions from the sbottom and stau sector [9]. On the other hand, the contribution from stop is proportional to $\cot\beta$ and it has more freedom

*cemsalihun@uludag.edu.tr
†ozerozdal@iyte.edu.tr

to satisfy the vacuum stability. In this context, the Higgs boson mass can be fed with the loop contributions from the stop sector, and it constrains the stop mass to the multi-TeV range, or it requires rather large mixing between stops. Even though it is possible to realize the stop of mass about top quark mass in the presence of the large mixing, the parameter space needs to be highly fine-tuned in this case [10]. The stop mass is bounded from below to a few hundred GeV if one imposes the fine-tuning condition [11].

Besides the Higgs boson results, another severe constraint comes from the observation of the rare decay $B_s \to \mu^+\mu^-$ with the branching ratio $\mathrm{BR}(B_s \to \mu^+\mu^-) = 3.2^{+1.5}_{-1.2} \times 10^{-9}$ [12]. This discovery is only another success of the SM, since its prediction for this rare decay more or less overlaps with the observation [13]. The small window in the prediction for this rare decay severely constrains the models for BSM. In the MSSM, the supersymmetric contributions to $B_s \to \mu^+\mu^-$ come from the charge parity (CP)-odd Higgs boson exchange, which is proportional to $(\tan\beta)^6/m_A^4$, where m_A is CP-odd Higgs boson mass. Accordingly, m_A needs to be heavy enough to suppress the $\tan\beta$ enhancement which requires $m_A \gtrsim 500$ GeV [14]. This constraint bounds the heavier CP-even Higgs boson mass (m_H) since $m_H \approx m_A$. After all, despite the abundance of the physical Higgs boson states, the MSSM cannot fit them in the mass range $m \lesssim 150$ GeV consistently with the experimental results, especially when it is constrained from M_{GUT}.

Considering the minimality it can be concluded from the discussion above that the MSSM may not cover the full story and one may consider some extension of the MSSM gauge group. One of the simplest extensions is imposing an extra $U(1)$ symmetry. Such an extension can be obtained from an underlying grand unified theory (GUT) theory involving a gauge group larger than $SU(5)$ [15]. Among the many different realizations of $G_{\mathrm{MSSM}} \times U(1)_X$, $U(1)_{B-L}$ provides a favorable framework, since the anomaly cancellation can be achieved by adding three MSSM singlets, and the right-handed neutrino is the first choice for such singlet fields. In this context, an anomaly free $U(1)_{B-L}$ extension of the MSSM provides a natural framework for the established nonzero neutrino masses [16] through the seesaw mechanisms. Besides, the invariance under $U(1)_{B-L}$ gauge group also imposes the R-parity conservation which is assumed in the MSSM to avoid fast proton decay. Hence, R-parity violation can be constrained by the smallness of the neutrino masses [17]. Moreover, R-parity conservation can be maintained if $U(1)_{B-L}$ symmetry is broken spontaneously [18]. Indeed, it was shown that $U(1)_{B-L}$ symmetry can be broken radiatively through a similar mechanism to the radiative electroweak symmetry breaking (REWSB) in the MSSM [19]. One can introduce a field whose nonzero vacuum expectation value (VEV) breaks the $U(1)_{B-L}$ symmetry. Hence, this field should carry $B-L$ charge and it is preferably singlet under the MSSM gauge group. If its $B-L$ charge is 2, then the R-parity conservation can be maintained. The holomorphy condition of the superpotential requires another MSSM singlet field whose $B-L$ charge is -2 in order to write the invariant Lagrangian under $U(1)_{B-L}$. Hence the MSSM extended by $U(1)_{B-L}$ (BLSSM) proposes two singlet Higgs fields ($\mathcal{X}_1$ and $\mathcal{X}_2$ with -2 and $+2$ B-L charges respectively) which can be counted for the observed anomalies in the Higgs decays at the mass scales other than ∼125 GeV.

The rest of the paper is organized as follows: In Sec. II we briefly describe the model with an emphasis on the Higgs sector. After we summarize the scanning procedure and the experimental constraints employed in our analysis in Sec. III, we present our results for the mass spectrum in Sec. IV. We also briefly mention leptogenesis in this section. In Sec. V we consider the Higgs boson decays into two photons and four leptons. Finally we summarize and conclude in Sec. VI.

II. MODEL DESCRIPTION

In this section, we review the BLSSM model with an emphasis on its Higgs sector. The superpotential in this model is given by

$$W = \mu H_u H_d + Y_u^{ij} Q_i H_u u_j^c + Y_d^{ij} Q_i H_d d_j^c + Y_e^{ij} L_i H_d e_j^c + Y_\nu^{ij} L_i H_u N_i^c + Y_N^{ij} N_i^c N_j^c \mathcal{X}_1 + \mu' \mathcal{X}_1 \mathcal{X}_2 \quad (1)$$

where the first line of Eq. (1) is the usual terms of the MSSM, while the second line includes the additional interactions from the right-handed neutrino N_i^c, and the singlet Higgs fields $\mathcal{X}_1$, $\mathcal{X}_2$ with -2 and $+2$ $B-L$ charges respectively. Once the model includes the right-handed neutrino, one can add a Yukawa interaction term for the neutrinos, and Y_ν stands for the Yukawa coupling for the neutrinos. Similarly, Y_N is the Yukawa coupling between N_i^c and $\mathcal{X}_1$. Finally μ'-term is the bilinear mixing between $\mathcal{X}_1$ and $\mathcal{X}_2$. The relevant soft supersymmetry breaking (SSB) Lagrangian is

$$-\mathcal{L}_{\not{\mathrm{SUSY}}} = -\mathcal{L}_{\not{\mathrm{SUSY}}}^{\mathrm{MSSM}} + m_{\tilde{N}^c}^2 |\tilde{N}^c|^2 + m_{\mathcal{X}_1}^2 |\mathcal{X}_1|^2 + m_{\mathcal{X}_2}^2 |\mathcal{X}_2|^2 + A_\nu \tilde{L} H_u \tilde{N}^c + A_N \tilde{N}^c \tilde{N}^c \mathcal{X}_1 + \frac{1}{2} M_{\tilde{B}'} \tilde{B}' \tilde{B}' + B(\mu' \mathcal{X}_1 \mathcal{X}_2 + \mathrm{H.c.}) \quad (2)$$

where $\mathcal{L}_{\not{\mathrm{SUSY}}}^{\mathrm{MSSM}}$ includes the SSB terms of MSSM, while the rest is associated with the $B-L$ symmetry. The meaning of the terms is similar to that in the MSSM. $m_{\tilde{N}^c}$, $m_{\mathcal{X}_1}$ and $m_{\mathcal{X}_2}$ are the SSB mass terms for the right-handed sneutrino, $\mathcal{X}_1$ and $\mathcal{X}_2$, while A_ν and A_N are the trilinear scalar interaction terms between the neutrinos and MSSM Higgs doublets and BLSSM Higgs singlets respectively. $M_{\tilde{B}'}$ is the SSB mass term for the gaugino $\tilde{B}'$ associated with the $B-L$

gauge group. Note that there exists a vector-boson partner Z' whose mass is severely constrained by the current experimental results ($m_{Z'} \gtrsim 2.5$ TeV).

Note that, in contrast to its nonsupersymmetry (non-SUSY) version, the BLSSM does not allow mixing between the doublet and singlet Higgs fields through the superpotential and SSB Lagrangian. Therefore, the Higgs potentials for these fields do not couple to each other. Then, the singlet Higgs potential can be written as

$$V(\mathcal{X}_1,\mathcal{X}_2) = \mu_1'^2|\mathcal{X}_1|^2 + \mu_2'^2|\mathcal{X}_2|^2 - \mu_3'(\mathcal{X}_1\mathcal{X}_2 + \text{H.c.}) + \frac{1}{2}g_{BL}^2(|\mathcal{X}_1|^2 - |\mathcal{X}_2|^2)^2 \quad (3)$$

where $\mu_1'^2 = m_{\mathcal{X}_1}^2 + \mu'^2$, $\mu_1'^2 = m_{\mathcal{X}_2}^2 + \mu'^2$, $\mu_3' = -B\mu'$ and g_{BL}^2 is the gauge coupling associated with the $B-L$ gauge group. Since the potential in Eq. (3) is in the same form as the MSSM Higgs potential, its minimization yields similar relations regarding the spontaneous breaking of $U(1)_{B-L}$ symmetry and the stability of the vacuum. When $m_{\mathcal{X}_1}$ or $m_{\mathcal{X}_2}$ (or both) is negative, the vacuum corresponds to nonzero VEVs $v'_{\mathcal{X}_1} = \langle\mathcal{X}_1\rangle$ and $v'_{\mathcal{X}_2} = \langle\mathcal{X}_2\rangle$.

A similar analysis in the REWSB can hold also for the $B-L$ symmetry breaking. The coupling Y_N between the right-handed neutrinos and $\mathcal{X}_1$ negatively contributes to $m_{\mathcal{X}_1}^2$, and if it is large enough, $m_{\mathcal{X}_1}^2$ can turn out to be negative from some positive values and it triggers the spontaneous $B-L$ symmetry breaking. It should be noted here that the interaction term between the right-handed neutrinos and $\mathcal{X}_1$ induces a Majorana mass term $-Y_N v'_{\mathcal{X}_1}\tilde{N}^c\tilde{N}^c$, which can destabilize the vacuum. For large values of Y_N, the global minimum can correspond to nonzero VEV of the right-handed sneutrinos, and hence it breaks the R parity [20]. Hence, Y_N should be large enough to trigger the spontaneous $B-L$ symmetry breaking, and small enough to preserve the R parity.

The spontaneous symmetry breaking mixes the fields and yields nondiagonal mass matrices. Since the two Higgs sectors are not coupled to each other, their mass square matrices can be diagonalized independently, and hence the mass eigenstates related to $\mathcal{X}_1$ and $\mathcal{X}_2$ remain singlet under the SM gauge group, but they can still participate in the interactions with the MSSM fields through loops. Figure 1 illustrates the effective Yukawa interactions between the singlet Higgs boson and matter particles. The top diagrams show the non-SUSY sector, while the bottom diagrams display the SUSY interference, since $\tilde{f}$, $\tilde{N}$, $\tilde{\chi}^0$ and $\tilde{\chi}^\pm$ stand for the sfermions, right-handed sneutrinos, neutralinos and charginos respectively. Since we assume that there is no mixing between the doublet and singlet Higgs fields, the singlet Higgs fields do not interact with the left-handed neutrinos. The top left diagram includes a Z' loop, and it is more likely suppressed due to the heavy mass bound on Z'. The contributions from the right top and bottom diagrams

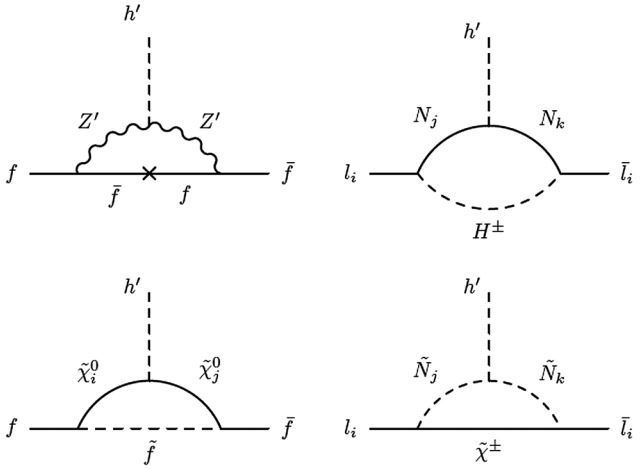

FIG. 1. The effective Yukawa interactions between the singlet Higgs and fermions. The top diagrams illustrate the non-SUSY loops, while the bottom diagrams display the SUSY interference.

depend on the mixing in the neutrino sector and Y_N. The supersymmetric contributions depend also on the sparticle masses running in the loops. The sneutrino loop is probably suppressed, since the sneutrino masses are at the order of TeV scale. The neutralino loop can lead to interesting results. Indeed, the contribution from the bottom left diagram depends on the $\tilde{B}'$ mass, which mixes with other neutralinos. Since there is no specific mass bound on $\tilde{B}'$, it can be as light as about 100 GeV, and it can even form the lightest neutralino [21].

Even though the discussion above shows that the singlet Higgs field can still alter the low scale phenomenology, it is rather a naive discussion, since the mixing between the Higgs fields is assumed not to be generated from another source or induced by the loop corrections. However, the invariance principle allows the Lagrangian to include a cross term between the strength tensors of gauge fields associated with the $U(1)$ gauge groups, $-\kappa_{ab}B^a_{\mu\nu}B^{b,\mu\nu}$, where $B_{\mu\nu}$ is the field strength tensor of a $U(1)$ gauge field, $a, b = Y, B-L$, the hypercharge and $B-L$ charge respectively; κ_{ab} is an antisymmetric tensor which includes the mixing of $U(1)_a$ and $U(1)_b$ gauge fields. This mixing couples the $B-L$ sector to the MSSM sector, and even if it is set to zero at M_{GUT}, it can be induced through RGEs [22]. In the case of nonzero gauge kinetic mixing, the gauge covariant derivative takes a noncanonical form as

$$\mathcal{D}_\mu = \partial_\mu - i(Y, B-L)\begin{pmatrix} g_Y & \tilde{g} \\ \tilde{g}' & g_{B-L} \end{pmatrix}\begin{pmatrix} B_\mu \\ B'_\mu \end{pmatrix} \quad (4)$$

where we have expressed the field in the flavor basis. Following the discussion in [23], we consider a basis by rotating the fields such that

$$\begin{pmatrix} g_Y & \tilde{g} \\ \tilde{g}' & g_{B-L} \end{pmatrix} \to \begin{pmatrix} g_1 & g_{YB} \\ 0 & g_4 \end{pmatrix}$$

where g_1 corresponds to the measured hypercharge coupling which is modified in BLSSM as given along with g_4 and g_{YB} in [23,24].

With nonzero mixing between the $U(1)$ gauge fields, a contribution from Z-boson loop similar to the top left diagram in Fig. 1 exists. On the other hand, the gauge kinetic mixing affects the mixing in the other sectors. Especially it induces a tree-level mixing between the MSSM doublet Higgs and BLSSM Higgs fields proportional to g_{YB}. As a consequence of nonzero gauge kinetic mixing, the two Higgs sectors become coupled and their mass square matrices should be diagonalized together. Then all the mass eigenstates couple to the MSSM particles at tree level. In this case the contributions in Fig. 1 represent the corrections to the tree-level couplings. Note that a nonzero mixing in the Higgs sector brings also contributions from the chargino loop. Having these extra Higgs bosons coupled to the MSSM particles leads to contributions to the observed processes associated with the Higgs sector. Interestingly these Higgs bosons can be counted for the excesses observed in the higher mass scales mentioned in the previous section.

Before concluding this section, we comment on the right-handed neutrino contributions to the Higgs bosons. As seen from Eq. (1), the presence of the right-handed neutrino allows one to have a Yukawa interaction term involved with H_u. This term yields contributions to the SM-like Higgs boson in addition to the stop sector, and it may relax the mass bound on the stops and consequently improve the fine-tuning in the model. However, after the electroweak symmetry breaking, this term induces a Dirac mass for the neutrinos. Smallness of the established neutrino masses strictly bounds the associated Yukawa coupling to very small ranges ($Y_\nu \lesssim 10^{-7}$), which strongly suppresses the contributions to the Higgs boson from the neutrino sector. Therefore the BLSSM and MSSM yield similar low scale phenomenology for the Higgs boson [25]. One can adopt the inverse seesaw mechanism into the BLSSM, which allows Y_ν to be at the order of unity [26]. Hence, the contribution from the right-handed neutrino sector to the Higgs boson cannot be neglected [27]. Besides, the singlet Higgs fields interact with another singlet field with nonzero $B-L$ charge along with the right-handed neutrino, which yields a significant contribution to masses of the extra Higgs bosons. Hence, in the presence of the inverse seesaw mechanism, it is not easy to fit at least one more Higgs boson to the scale $m_h \lesssim 150$ GeV, when the model is constrained from $M_{\rm GUT}$. In other words, seeking the second Higgs boson of mass less than 150 GeV leads also to a very light SM-like Higgs boson ($\ll 125$ GeV). Note that even in the BLSSM without inverse seesaw, the right-handed neutrino sector is still effective on the singlet Higgs boson masses, but since the SM-like Higgs boson does not acquire significant contributions from right-handed neutrinos, the singlet Higgs boson mass can be found light without affecting the SM-like Higgs boson mass. The RGEs for the singlet Higgs fields and the right-handed neutrino from $M_{\rm GUT}$ to the low scale are [19]

$$\frac{dm^2_{\chi_1}}{dt} = \frac{1}{16\pi^2}[6g_{BL}M^2_{BL} - 2Y_N(m^2_{\chi_1} + 2m^2_N + A^2_N)] \quad (5a)$$

$$\frac{dm^2_{\chi_2}}{dt} = \frac{1}{16\pi^2}6g_{BL}M^2_{BL} \quad (5b)$$

$$\frac{dm^2_N}{dt} = \frac{1}{16\pi^2}\left[\frac{3}{2}g_{BL}M^2_{BL} - Y_N(m^2_{\chi_1} + 2m^2_N + A^2_N)\right] \quad (6)$$

where $t = \log(Q)$ and Q is an energy scale between the low scale and the GUT scale.

III. SCANNING PROCEDURE AND EXPERIMENTAL CONSTRAINTS

We have employed SPheno 3.3.3 package [28] obtained with SARAH 4.5.8 [29]. In this package, the weak scale values of the gauge and Yukawa couplings present in the MSSM are evolved to the unification scale $M_{\rm GUT}$ via the RGEs. $M_{\rm GUT}$ is determined by the requirement of the gauge coupling unification through their RGE evolutions. Note that we do not strictly enforce the unification condition $g_1 = g_2 = g_3$ at $M_{\rm GUT}$ since a few percent deviation from the unification can be assigned to unknown GUT-scale threshold corrections [30]. With the boundary conditions given at $M_{\rm GUT}$, all the SSB parameters along with the gauge and Yukawa couplings are evolved back to the weak scale. Note that the gauge coupling associated with the $B-L$ symmetry is determined by the unification condition at the GUT scale by imposing $g_1 = g_2 = g_4 \approx g_3$.

The requirement of REWSB [31] puts an important theoretical constraint on the parameter space. In our case, also the radiative $B-L$ symmetry breaking is required, but this requirement constrains rather the right-handed neutrino sector and the coupling Y_N to the $B-L$ singlet Higgs fields.

We have performed random scans over the following parameter space,

$$\begin{aligned} &0 \le m_0 \le 3 \text{ (TeV)} \\ &0 \le M_{1/2} \le 5 \text{ (TeV)} \\ &1.2 \le \tan\beta \le 60 \\ &-3 \le A_0/m_0 \le 3 \\ &\mu > 0, \quad \mu' > 0, \quad m_t = 173.3 \text{ GeV}, \end{aligned} \quad (7)$$

where we restrict ourselves only to the universal boundary conditions in which m_0 denotes the SSB mass term for all

the scalars including the MSSM doublet and BLSSM singlet Higgs fields, while $M_{1/2}$ stands for the SSB mass terms for the gauginos including one associated with the $U(1)_{B-L}$ gauge group. A_0 is the SSB trilinear scalar interacting term; $\tan\beta$ is the ratio of VEVs of the MSSM Higgs doublets. Note that the ratio of VEV of the BLSSM singlet Higgs fields is, in principle, a free parameter. In our scan it is restricted to be approximately unity ($\tan\beta' \equiv v_{\chi_1}/v_{\chi_2} \approx 1-1.2$). Besides, μ is the bilinear mixing of the MSSM doublet Higgs fields, while μ' is of the BLSSM singlet Higgs fields. In addition, m_t is the top quark mass and we set it to its central value [32]. Note that the sparticle spectrum is not too sensitive to one or two sigma variation in the top quark mass [33], but it can shift the Higgs boson mass by 1–2 GeV [34]. Finally, we also vary g_{YB} in the perturbative level, while we fix $Y_N \approx 0.4$. Note that Y_N is determined at the low scale, and its values larger than about 0.4 can yield Landau pole below the GUT scale [23].

In scanning the parameter space, we use our interface which employs the Metropolis-Hasting algorithm as described in [35]. All the data points satisfy the requirement of REWSB. After collecting the data, we impose the mass bounds on all the particles [36] and the constraints from the rare B-boson decays such as $B_s \to \mu^+\mu^-$ [12], $b \to s\gamma$ [37], and $B_u \to \tau\nu$ [38] as follows:

$$m_h = 123 - 127 \text{ GeV} \tag{8}$$

$$m_{\tilde{g}} \geq 1.8 \text{ TeV} \tag{9}$$

$$m_{\tilde{\tau}} \geq 105 \text{ GeV} \tag{10}$$

$$0.8 \times 10^{-9} \leq \text{BR}(B_s \to \mu^+\mu^-) \leq 6.2 \times 10^{-9}(2\sigma) \tag{11}$$

$$2.99 \times 10^{-4} \leq \text{BR}(b \to s\gamma) \leq 3.87 \times 10^{-4}(2\sigma) \tag{12}$$

$$0.15 \leq \frac{\text{BR}(B_u \to \tau\nu_\tau)_{\text{MSSM}}}{\text{BR}(B_u \to \tau\nu_\tau)_{\text{SM}}} \leq 2.41(3\sigma) \tag{13}$$

where we emphasize the updated mass bounds on the Higgs boson mass [1,2], and the gluino mass [39], since they have been updated by the current LHC results. In addition, we highlight the LEPII bound on stau mass [36], since we allow it to be lighter than neutralino in our work.

In addition to those mentioned above, another constraint implied from the dark matter (DM) observations significantly limits the parameter space. It requires the lightest supersymmetric particle (LSP) to be stable and of no electric or color charge, which excludes the regions leading to $\tilde{\tau}$ or $\tilde{t}$ LSP solutions. On the other hand, even if a solution does not satisfy the DM observations, it can still survive in conjunction with other form(s) of DM [40]. Therefore, we do not impose the DM constraints in our scan and we do not require the solutions to yield neutralino LSP.

Before concluding the constraints, which we impose in our results, we should note the muon anomalous magnetic moment (muon $g-2$). As is known, the SM prediction on the muon $g-2$ [41] deviates from the experimental measurements [42] at about 3σ. If SUSY is a solution to the muon $g-2$, the SUSY particles, namely, smuon and weak gaugino (bino or wino) masses, should be around a few hundred GeV, in order to utilize the supersymmetric contributions [43]. However, the observation of the Higgs boson of mass about 125 GeV requires rather heavy sparticle spectrum within the MSSM framework, and it results in a strong tension in simultaneous resolution for both the 125 GeV Higgs boson and the muon $g-2$ problem since SUSY contributions to muon $g-2$ are suppressed by the heavy spectrum. Nonuniversality in gaugino and/or scalar masses may remove this tension [44]. Since we imposed universal boundary conditions in our work, we did not expect to resolve the muon $g-2$ problem, because the BLSSM yields similar phenomenology to the MSSM in the Higgs sector. Hence, we only require the solutions to do no worse than the SM in regard to muon $g-2$ by imposing $3.4 \times 10^{-10} \leq \Delta a_\mu \leq 55.6 \times 10^{-10}$ [42], where $\Delta a_\mu \equiv 1/2(g-2)_\mu^{\text{SUSY}} - 1/2(g-2)_\mu^{\text{SM}}$.

IV. MASS SPECTRUM IN BLSSM PARAMETER SPACE

In this section, we present the results for the mass spectrum obtained from the scan over the parameter space given in Eq. (7). Figure 2 displays the regions with plots in $m_0 - M_{1/2}$, $m_0 - A_0/m_0$, $m_0 - \tan\beta$, and $g_{YB}(\text{GUT}) - g_{YB}(\text{SUSY})$ planes. All points are consistent with REWSB. Gray points are excluded by the current LHC results, even though they yield physical solutions, while green points satisfy the mass bounds and constraints from the rare B decays mentioned in the previous section. Blue points form a subset of green, and they represent solutions with $m_{h_2} \leq 150$ GeV. As seen from the $m_0 - M_{1/2}$ plane, the condition for the second Higgs boson lighter than 150 GeV (blue) excludes a significant portion of the LHC allowed region (green). For $M_{1/2} \sim 1$ TeV, m_0 is restricted to a narrow range at about 500 GeV, and this range opens up to 2 TeV for heavier gaugino masses. This interplay can be partially understood with the heavy gaugino effect on the singlet Higgs mass. Even though it has very light masses at the GUT scale, the singlet Higgs boson mass is raised by the heavy M_{B-L} such that $m_{h_2} \lesssim 150$ GeV. On the other hand, for the large values of m_0, which means heavy m_{χ_1} and m_N, as seen from Eq. (5a), these masses reduce the singlet Higgs boson mass. The results in the $m_0 - M_{1/2}$ plane show that m_0 reaches its highest values when $m_0 \approx M_{1/2} \sim 2$ TeV. On the other hand, the $m_0 - A_0/m_0$ panel shows that the heavy gaugino mass cannot explain the results fully, the regions with larger m_0 values require a positive SSB trilinear scalar interaction term and

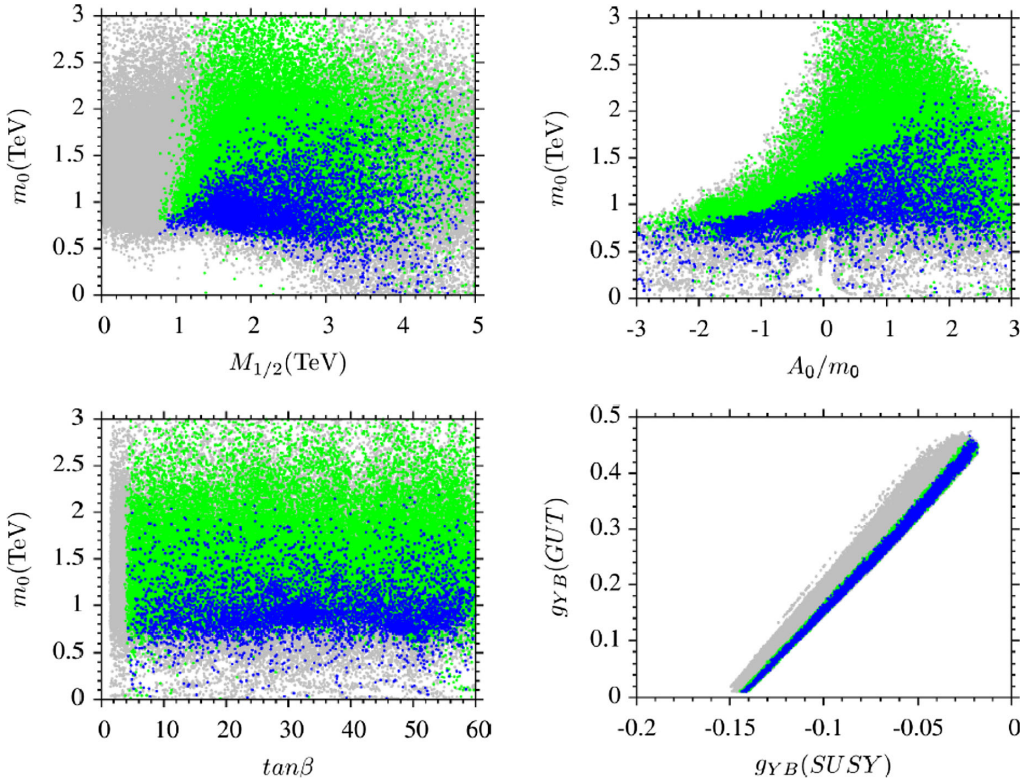

FIG. 2. Plots in $m_0 - M_{1/2}$, $m_0 - A_0/m_0$, $m_0 - \tan\beta$, and $g_{YB}(\mathrm{GUT}) - g_{YB}(\mathrm{SUSY})$ planes. All points are consistent with REWSB. Gray points are excluded by the current LHC results, even though they yield physical solutions, while green points satisfy the mass bounds and constraints from the rare B decays mentioned in the previous section. Blue points form a subset of green, and they represent solutions with $m_{h_2} \leq 150$ GeV.

when $A_0/m_0 \gtrsim 1.5$, m_0 can be as large as 2 TeV and the solutions can still yield two Higgs bosons with mass ≤ 150 GeV. When A_0 is negative, the RGE evolution of A_N has an increasing slope, and its contribution to the singlet Higgs boson takes over the heavy gaugino effect. Therefore the solutions with large A_N needs to be restricted with the low m_0 and $M_{1/2}$ values. The $m_0 - \tan\beta$ plane shows that it is possible to find solutions with $m_{h_2} \leq 150$ GeV for almost all values of $\tan\beta$. Finally the $g_{YB}(\mathrm{GUT}) - g_{YB}(\mathrm{SUSY})$ plane represents our results in regard to the gauge kinetic mixing. Even though we vary it in the perturbative level at the GUT scale, its low scale value is found in the range $(-0.15 - 0)$.

In Fig. 3 we present our results in the $M_{\mathrm{SUSY}} - v_X$, $m_{N_2} - m_{N_1}$, $M_{\tilde{N}_1} - v_X$, and $m_{\tilde{N}_2} - m_{\tilde{N}_1}$ planes. The color coding is the same as Fig. 2. The solid line in the $M_{\mathrm{SUSY}} - v_X$ plane indicates the regions where $M_{\mathrm{SUSY}} = v_X$. According to our results, the breaking of $U(1)_{B-L}$ happens at about $v_X \approx 5$ TeV. Since $U(1)_{B-L}$ is no more the symmetry in the model, the existence of the right-handed neutrinos can trigger baryon and lepton number violating processes, which can be considered as a source for the baryon asymmetry in the Universe. Assuming that the supersymmetric particles all decouple below M_{SUSY}, the $M_{\mathrm{SUSY}} - v_X$ plane shows that $U(1)_{B-L}$ symmetry breaking can be realized in both the supersymmetric regime ($v_X > M_{\mathrm{SUSY}}$) and nonsupersymmetric regime ($v_X < M_{\mathrm{SUSY}}$). In the nonsupersymmetric regime, the baryon and lepton violating processes rely on the right-handed neutrinos. Since the Yukawa coupling associated with the neutrinos is very small ($Y_\nu \sim 10^{-7}$), the thermal leptogenesis can provide sufficient baryon asymmetry when the right-handed neutrinos are degenerate in mass [25,45]. As shown in the $m_{N_2} - m_{N_1}$ plane, the right-handed neutrino masses ($\sim 1.7 - 2.2$ TeV) are nearly degenerate. In addition to the right-handed neutrinos, the sneutrino antisneutrino can be counted as another source in the supersymmetric regime [46]. After the right-handed neutrinos decouple, $B - L$ symmetry is restored globally.

Figure 4 represents the results for the sparticle mass spectrum with plots in $m_{\tilde{t}_1} - m_{\tilde{\chi}_1^0}$, $m_{\tilde{b}_1} - m_{\tilde{\chi}_1^0}$, $m_{\tilde{\chi}_1^\pm} - m_{\tilde{\chi}_1^0}$ and $m_{\tilde{\tau}_1} - m_{\tilde{\chi}_1^0}$ planes. The color coding is the same as Fig. 2. In addition, the solid line shows the degenerate mass region in each plane. As is seen from the $m_{\tilde{t}_1} - m_{\tilde{\chi}_1^0}$ and $m_{\tilde{b}_1} - m_{\tilde{\chi}_1^0}$ planes, $m_{\tilde{t}_1} \gtrsim 1$ and $m_{\tilde{b}_1} \gtrsim 1.5$ TeV, and these masses are mostly required to realize the SM-like Higgs boson mass at about 125 GeV. Moreover, the $m_{\tilde{\chi}_1^\pm} - m_{\tilde{\chi}_1^0}$ plane shows that the lightest chargino cannot be lighter than 600 GeV. Even though we do not require the neutralino to

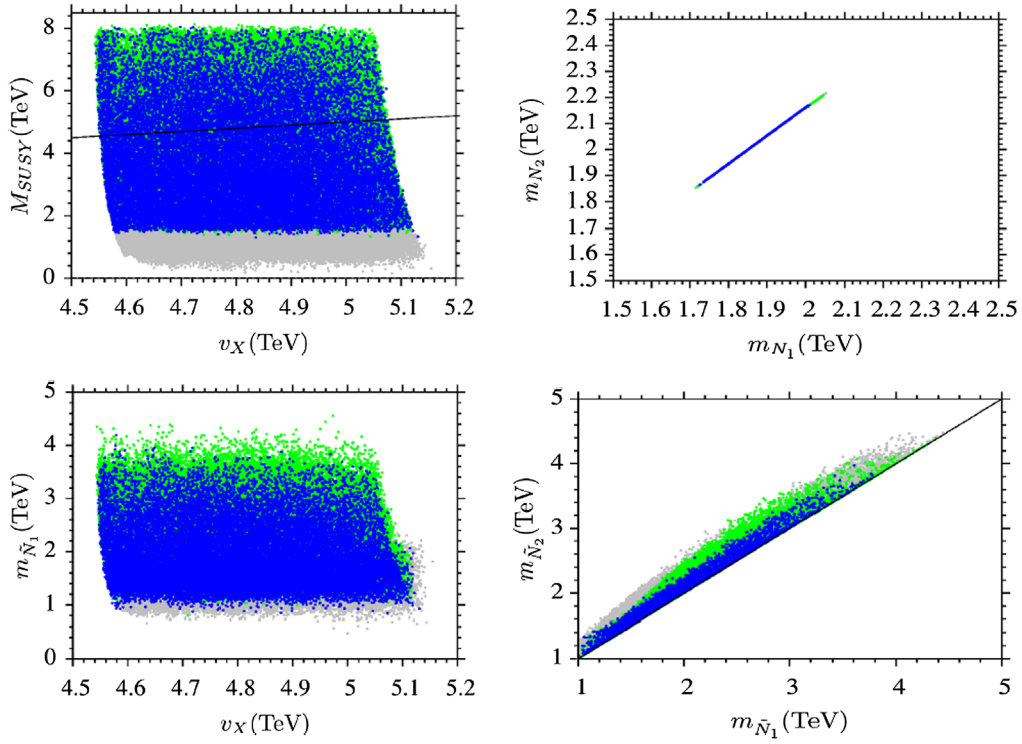

FIG. 3. Plots in the $M_{\rm SUSY}-v_X$, $m_{N_2}-m_{N_1}$, $M_{\tilde{N}_1}-v_X$, and $m_{\tilde{N}_2}-m_{\tilde{N}_1}$ planes. The color coding is the same as Fig. 2. The solid line in the $M_{\rm SUSY}-v_X$ plane indicates the regions where $M_{\rm SUSY}=v_X$.

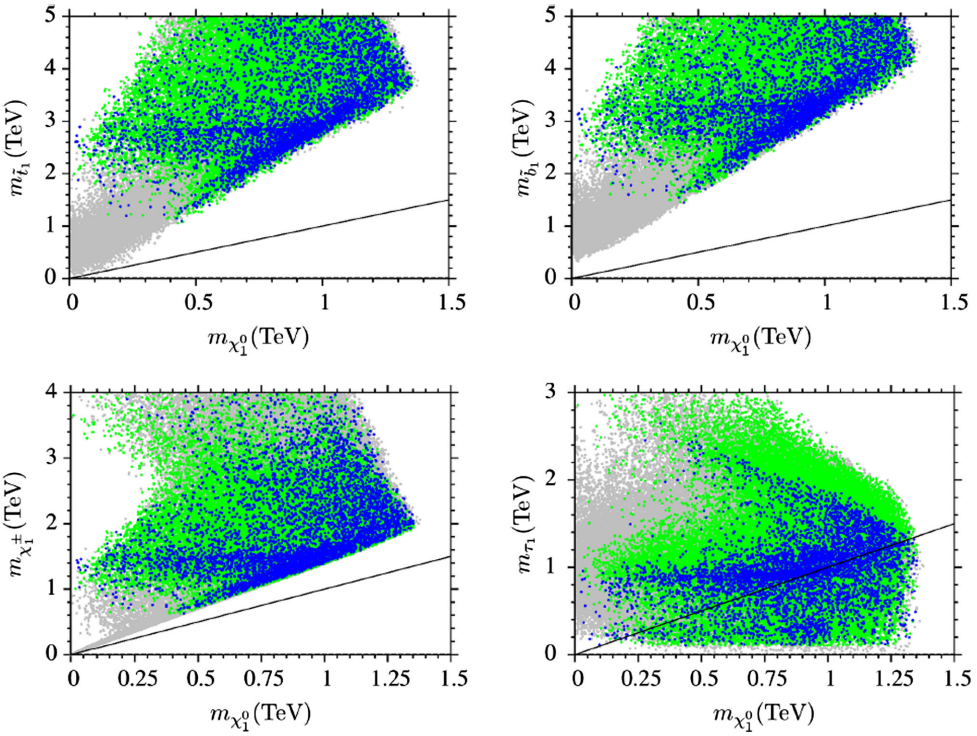

FIG. 4. Plots in $m_{\tilde{t}_1}-m_{\tilde{\chi}_1^0}$, $m_{\tilde{b}_1}-m_{\tilde{\chi}_1^0}$, $m_{\tilde{\tau}_1}-m_{\tilde{\chi}_1^0}$, and $m_{\tilde{\chi}_1^\pm}-m_{\tilde{\chi}_1^0}$ planes. The color coding is the same as Fig. 2. In addition, the solid line shows the degenerate mass region in each plane.

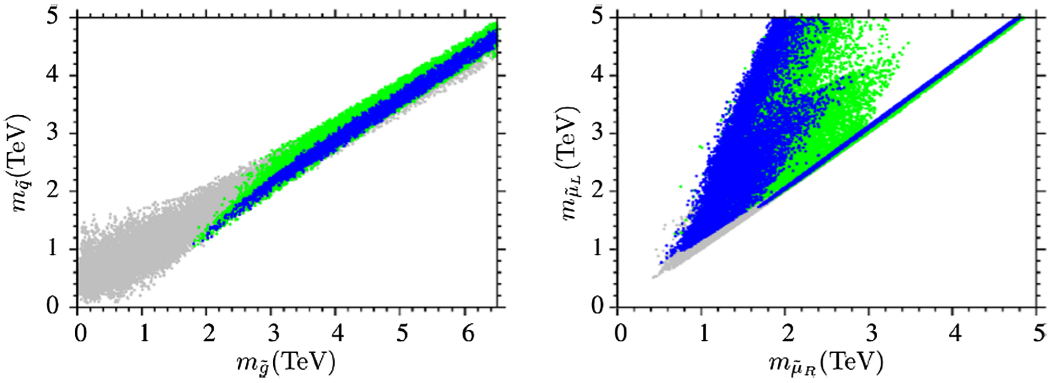

FIG. 5. Plots in $m_{\tilde{q}} - m_{\tilde{g}}$ and $m_{\tilde{\mu}_L} - m_{\tilde{\mu}_R}$ planes. The color coding is the same as Fig. 2.

be the LSP, it is found to be much lighter than other sparticles except stau. The $m_{\tilde{\tau}_1} - m_{\tilde{\chi}_1^0}$ plane represents the stau mass along with the neutralino mass, and it can be lighter than neutralino as well as being much heavier. One can constrain the stau mass further by the prompt decay of stau to gravitino in the case of gravitino LSP [47].

We continue with Fig. 5 to present our results for the sparticle spectrum with plots in $m_{\tilde{q}} - m_{\tilde{g}}$ and $m_{\tilde{\mu}_L} - m_{\tilde{\mu}_R}$ planes. The color coding is the same as Fig. 2. The $m_{\tilde{q}} - m_{\tilde{g}}$ shows that the squarks from the first two families and gluino should be heavier than 2 TeV. Even though we impose a mass bound on gluino at about 1.8 TeV, the other LHC results mentioned in Sec. III constrain gluino mass further to about 2 TeV (green). Imposing the condition that $m_{h_2} \leq 150$ GeV (blue) does not constrain the gluino or squark masses strictly. Similarly the results for the smuon masses are represented in the $m_{\tilde{\mu}_L} - m_{\tilde{\mu}_R}$ plane. According to our results, the lightest left- and right-handed smuon masses are about 1 TeV. In this case, one can expect a relatively better result for the muon anomalous magnetic moment (muon $g-2$), but since the supersymmetric contributions are more or less suppressed by the smuon masses, the results for the muon $g-2$ hardly reach to the 2σ band of the experimental results.

Finally we display our results for the mass spectrum of the Higgs bosons in Fig. 6 with plots in $m_{h_2} - m_{h_1}$ and $m_{h_3} - m_{A_1}$ planes. The color coding is the same as Fig. 2 except that the Higgs mass bound in green is not applied in the $m_{h_2} - m_{h_1}$ since m_{h_1} is plotted in one axis. The diagonal line represents the mass degeneracy. The $m_{h_2} - m_{h_1}$ plane shows that there are plenty of solutions with m_{h_1}, $m_{h_2} \leq 150$ GeV. Moreover, following the diagonal line we can see that it is also possible to find the lightest two Higgs bosons that are almost degenerate at about $m_{h_1} \approx m_{h_2} \sim 125$ GeV. The other Higgs bosons are found to be rather heavy ($\gtrsim$1 TeV) as shown in the $m_{h_3} - m_{A_1}$ plane.

V. HIGGS DECAYS

We have represented the mass spectrum in the BLSSM in the previous section. As mentioned, the BLSSM provides an extra Higgs boson which can be lighter than 150 GeV, and even two Higgs bosons can be degenerate at about 125 GeV. With the mixing between two Higgs fields this region can provide a relatively rich phenomenology for the Higgs decays. In this section, we present our results for the Higgs decays in two photons and four leptons.

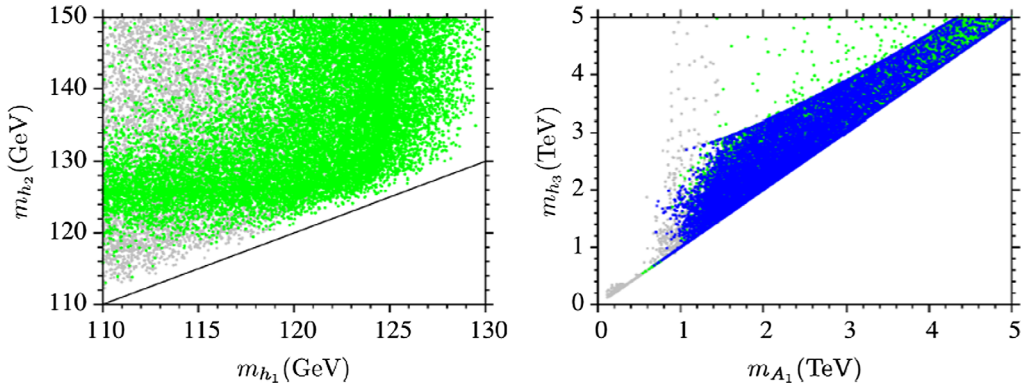

FIG. 6. Plots in $m_{h_2} - m_{h_1}$ and $m_{h_3} - m_{A_1}$ planes. The color coding is the same as Fig. 2 except that the Higgs mass bound in green is not applied in the $m_{h_2} - m_{h_1}$ plane since m_{h_1} is plotted in one axis. The diagonal line represents the mass degeneracy.

A. $h \to \gamma\gamma$

The sparticles shown in Fig. 4 contribute to the loop induced coupling between the Higgs boson and two photons in SUSY models. Since their contributions are inversely proportional to their masses, the contributions from stop and sbottom are suppressed by their heavy masses. The main contribution comes from the stau, since its mass can be as low as 100 GeV. In addition, chargino contribution can be counted as a correction. Moreover, since the second Higgs boson mass lighter than 150 GeV can be realized, there is also an induced coupling between h_2 and two photons. One can quantify the excess relative to the SM prediction in $h \to \gamma\gamma$ with the parameter $R^i_{\gamma\gamma}$ defined as

$$R^i_{\gamma\gamma} = \frac{\sigma(pp \to h_i) \times \mathrm{BR}(h_i \to \gamma\gamma)}{\sigma(pp \to h)_{\mathrm{SM}} \times \mathrm{BR}(h \to \gamma\gamma)_{\mathrm{SM}}} \qquad (14)$$

where $\sigma(pp \to h_i)$ denotes the production cross section of the Higgs boson h_i, and $\mathrm{BR}(h_i \to \gamma\gamma)$ is the branching ratio of the process in which the Higgs boson decays into two photons. The definitions for the terms in the denominator are the same, but they represent the SM predictions for the same process.

Equation (14) reveals the importance of the Higgs boson production at the LHC as well as the loop induced coupling between the Higgs bosons and photons. Since the Higgs boson couplings to the matter fields in the first two families are negligible, the main contributions to $\sigma(pp \to h_i)$ come from GGF, vector boson fusion (VBF), associated vector boson-Higgs production and Higgs production along with the top quark pair. Figure 7 displays plots for the Higgs boson production cross section through GGF (top panel) and VBF (bottom panel) in the $\sigma(gg \to h_1) - m_{h_1}$, $\sigma(VB \to h_1) - m_{h_1}$, $\sigma(gg \to h_2) - m_{h_2}$ and $\sigma(VB \to h_2) - m_{h_2}$ planes. The color coding is the same as Fig. 2, except we do not apply the SM Higgs boson constraint ($m_{h_1} \sim 125$ GeV) to the left panel, since m_{h_1} is directly plotted here. Similarly,the condition $m_{h_2} \leq 150$ GeV, represented by the blue region, is not applied to the right panels, since m_{h_2} is on the horizontal axis. As seen from the plots of Fig. 7, GGF dominates in the Higgs boson production at the LHC as happened for the SM Higgs boson. However, while GGF yields a production cross section of the order about 10^2 pb in the SM [48] and MSSM [49], in the BLSSM the GGF cross section is found at about 20 pb at most. This is because the Higgs boson couplings are diminished by $\sin\alpha$ and $\cos\alpha$, where α measures the mixing between the Higgs fields. As shown in

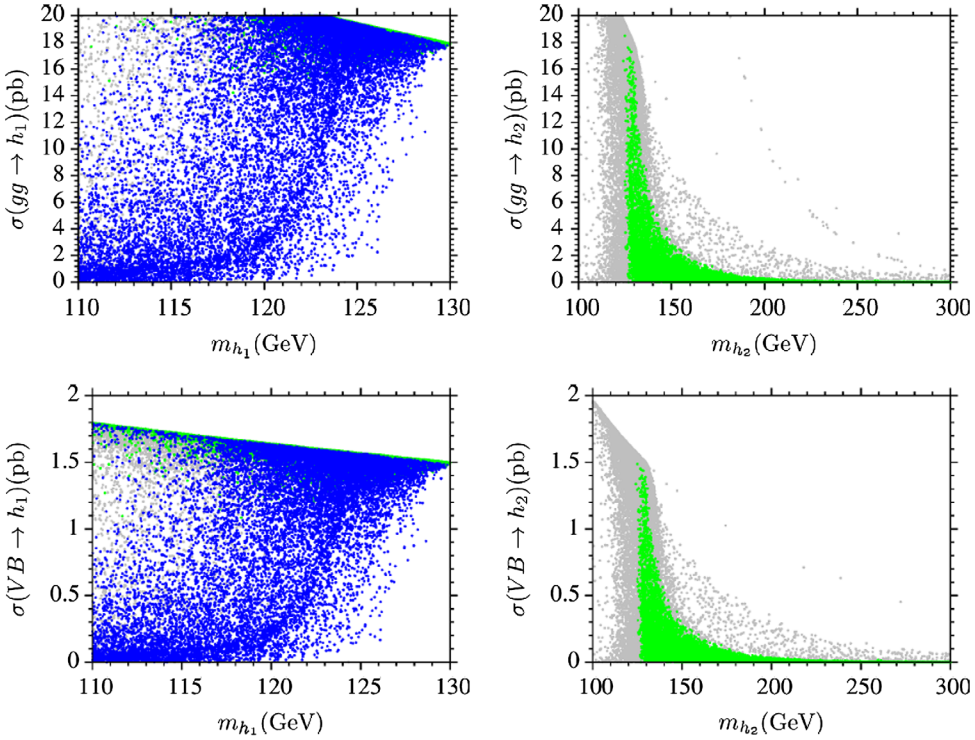

FIG. 7. Plots for the Higgs boson production cross section through gluon fusion (GGF) (top panel) and vector boson fusion (VBF) (bottom panel) in the $\sigma(gg \to h_1) - m_{h_1}$, $\sigma(VB \to h_1) - m_{h_1}$, $\sigma(gg \to h_2) - m_{h_2}$ and $\sigma(VB \to h_2) - m_{h_2}$ planes. The color coding is the same as Fig. 2, except we do not apply the SM Higgs boson constraint ($m_{h_1} \sim 125$ GeV) to the left panel, since m_{h_1} is directly plotted here. Similarly, the condition $m_{h_2} \leq 150$ GeV, represented by the blue region, is not applied to the right panels, since m_{h_2} is on the horizontal axis.

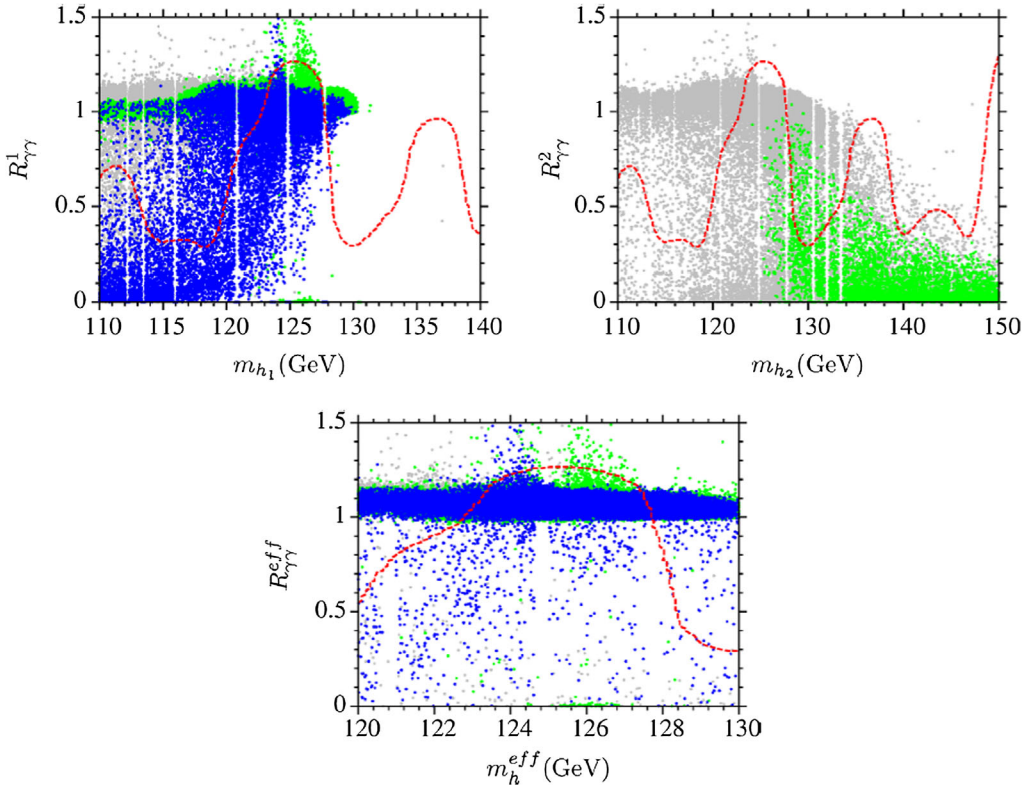

FIG. 8. Plots in $R^1_{\gamma\gamma} - m_{h_1}$, $R^2_{\gamma\gamma} - m_{h_2}$ and $R^{\rm eff}_{\gamma\gamma} - m^{\rm eff}_h$ planes. The color coding is the same as Fig. 7. The red dashed line indicates the observed cross section in $h \to \gamma\gamma$ normalized to the SM prediction [6].

the $\sigma(gg \to h_1) - m_{h_1}$ plane, h_1 behaves mostly like the SM Higgs boson, while h_2 can share this behavior when $m_{h_2} \lesssim 150$ GeV. As seen from the $\sigma(gg \to h_2) - m_{h_2}$ plane, the h_2 production has a sharp fall for relatively heavier mass scales, and finally it drops to zero for $m_{h_2} \gtrsim 200$ GeV. It is because the second lightest Higgs boson is mostly formed by the BLSSM Higgs fields, which are SM singlets, as the mass difference between the two lightest Higgs bosons increases. A similar discussion can hold for the VBF as shown in the bottom plane of Fig. 7. VBF is usually the production channel with the second larger contribution, and it is one order of magnitude smaller than the GGF results.

We present our results for the possible excesses in $h_i \to \gamma\gamma$ in Fig. 8 with plots $R^1_{\gamma\gamma} - m_{h_1}$, $R^2_{\gamma\gamma} - m_{h_2}$ and $R^{\rm eff}_{\gamma\gamma} - m^{\rm eff}_h$ planes. The color coding is the same as Fig. 7. The red dashed line indicates the observed cross section in $h \to \gamma\gamma$ normalized to the SM prediction [6]. As seen from the $R^1_{\gamma\gamma} - m_{h_1}$ plane, the BLSSM yields plenty of solutions which can feed the excess in $h \to \gamma\gamma$ for both $m_{h_2} \leq 150$ GeV (blue) and $m_{h_2} \geq 150$ GeV (green). These solutions can be explained by effects of the light staus and relatively light charginos as shown in Fig. 4. In addition to the light sparticles, also the second lightest Higgs boson mass can be realized as nearly degenerate with $m_{h_1} \approx 125$ GeV, and it can be seen from the $R^2_{\gamma\gamma} - m_{h_2}$ plane that it can provide some cross section in $h \to \gamma\gamma$ as much as the SM ($R^2_{\gamma\gamma} \sim 1$). In this region, we have two Higgs bosons of mass about 125 GeV, and both contribute to the cross section of $h \to \gamma\gamma$. If we define $m^{\rm eff}_h$ and $R^{\rm eff}_{\gamma\gamma}$ as

$$m^{\rm eff}_h = \frac{m_{h_1} R^1_{\gamma\gamma} + m_{h_2} R^2_{\gamma\gamma}}{R^1_{\gamma\gamma} + R^2_{\gamma\gamma}}, \qquad R^{\rm eff}_{\gamma\gamma} = R^1_{\gamma\gamma} + R^2_{\gamma\gamma} \tag{15}$$

the predicted effective cross section by many solutions is lifted up to a region where $R^{\rm eff}_{\gamma\gamma} \gtrsim 1$ for $m^{\rm eff}_h \sim 125$ GeV, as seen from the $R^{\rm eff}_{\gamma\gamma} - m^{\rm eff}_h$ plane.

Before concluding this section, it should be noted that the second lightest Higgs boson can be accounted for the other peaks at about 137 and 145 GeV observed in the experiments [6]. As seen from the $R^2_{\gamma\gamma} - m_{h_2}$ panel, the solutions may relatively provide some nonzero cross sections at these mass scales. However, the solutions around the second peak at 137 GeV are excluded by the Higgs boson constraint. Since we have restricted ourselves with the universal boundary conditions at $M_{\rm GUT}$, these predictions can be ameliorated by imposing nonuniversality.

B. $h \to 4l$

A similar discussion can be followed for the process in which the Higgs boson decays into four leptons. In the SM,

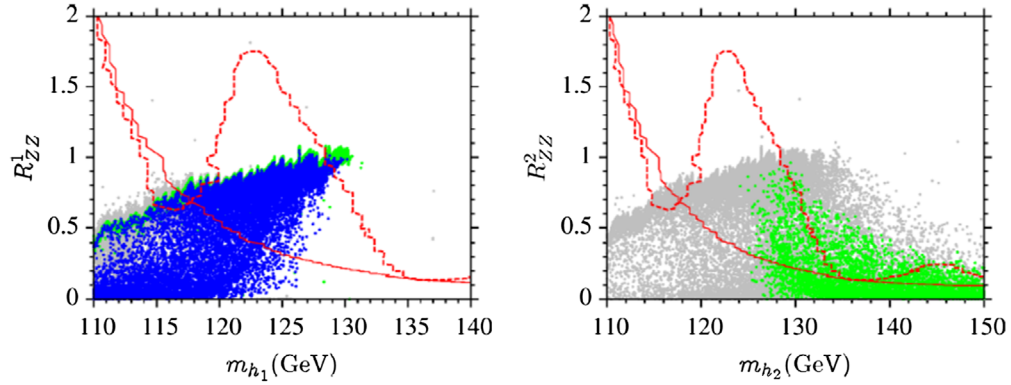

FIG. 9. Plots in $R^1_{ZZ}-m_{h_1}$ and $R^2_{ZZ}-m_{h_2}$. The color coding is the same as Fig. 7. The dashed line indicates the observed cross section, while the solid line represents the expected cross section without the Higgs boson [7].

this process is mediated via two Z-bosons, each of which eventually decays into a lepton pair. In the BLSSM, such decays can include also Z', but due to its heavy mass ($m_{Z'}=2.5$ TeV in our work), such processes are highly suppressed. Hence, the difference in $h\to 4l$ between the BLSSM and the observation basically comes from the Higgs boson decays into two Z-bosons. Figure 9 represents our results with plots in $R^1_{ZZ}-m_{h_1}$ and $R^2_{ZZ}-m_{h_2}$. The color coding is the same as Fig. 7. The dashed line indicates the observed cross section, while the solid line represents the expected cross section without the Higgs boson [7]. In contrast to the Higgs decays into two photons, the BLSSM's predictions can be only as good as ones in the SM, even in the case of the degenerate Higgs bosons. On the other hand, if one considers the second peak observed at $m_h\sim 145$ GeV, it can be seen from the $R^2_{ZZ}-m_{h_2}$ plane, the second Higgs boson can nicely fill the region around this peak.

VI. CONCLUSION

We presented the predictions on the mass spectrum and Higgs boson decays in the BLSSM framework with universal boundary conditions. We briefly mentioned the right-handed neutrino sector. The radiative breaking of $U(1)_{B-L}$ symmetry happens at about 5 TeV below which $B-L$ is no more the conserved symmetry and the right-handed neutrinos can trigger baryon and lepton number violating process till they decouple from the SM sector at 1.7–2.2 TeV. Radiative breaking of $B-L$ symmetry can happen in both supersymmetric ($v_X > M_{\rm SUSY}$) and nonsupersymmetric ($v_X < M_{\rm SUSY}$). The sneutrino-antisneutrino mixing can be counted as another source for baryon and lepton asymmetry in the Universe.

We found the stop and sbottom masses heavier than 1.5 TeV, and gluino mass greater than 2 TeV. The color sector is required to be heavy in order to realize the SM-like Higgs boson consistent with the observations. Even though the BLSSM's predictions for the Higgs boson are similar to the MSSM, it predicts another Higgs boson, which can be lighter than 150 GeV, and even degenerate with the lightest CP-even Higgs boson at about 125 GeV. Besides light staus ($\gtrsim$100 GeV), the second Higgs boson also contributes to the Higgs decay processes in the presence of gauge kinetic mixing. We showed that the excess in $h\to\gamma\gamma$ at about 125 GeV mass scale can be realized. The solutions which can provide an excess at 137 and 145 GeV in this process are rather excluded by the 125 GeV Higgs boson constraint. Such solutions can be cured by considering nonuniversal boundary conditions in the BLSSM. In addition, we concluded that the BLSSM predictions for $h\to 4l$ are only as good as the SM, but it is eligible to fit the second excess at about 145 GeV.

ACKNOWLEDGMENTS

We thank Durmus Ali Demir and Shaaban Khalil for useful discussions and comments. This work is supported by the Scientific and Technological Research Council of Turkey (TUBITAK) Grant No. MFAG-114F461. C. S. U. acknowledges the support of H2020-MSCA-RISE-2014 Grant No. 645722 (NonMinimalHiggs), with which some parts of this work were completed at the University of Southampton. This work used Extreme Science and Engineering Discovery Environment (XSEDE), which is supported by the National Science Foundation Grant No. OCI-1053575. Part of the numerical calculations reported in this paper were performed at the National Academic Network and Information Center (ULAKBIM) of TUBITAK, High Performance and Grid Computing Center (TRUBA resources).

[1] G. Aad *et al.* (ATLAS Collaboration), Observation of a new particle in the search for the standard model Higgs boson with the ATLAS detector at the LHC, Phys. Lett. B **716**, 1 (2012).

[2] S. Chatrchyan *et al.* (CMS Collaboration), Observation of a new boson at a mass of 125 GeV with the CMS experiment at the LHC, Phys. Lett. B **716**, 30 (2012).

[3] E. Gildener, Gauge symmetry hierarchies, Phys. Rev. D **14**, 1667 (1976); Gauge symmetry hierarchies revisited, Phys. Lett. **92B**, 111 (1980); S. Weinberg, Gauge hierarchies, Phys. Lett. **82B**, 387 (1979); L. Susskind, Dynamics of spontaneous symmetry breaking in the Weinberg-Salam theory, Phys. Rev. D **20**, 2619 (1979); M. J. G. Veltman, The infrared-ultraviolet connection, Acta Phys. Pol. B **12**, 437 (1981).

[4] G. Degrassi, S. Di Vita, J. Elias-Miro, J. R. Espinosa, G. F. Giudice, G. Isidori, and A. Strumia, Higgs mass and vacuum stability in the standard model at NNLO, J. High Energy Phys. 08 (2012) 098; F. Bezrukov, M. Y. Kalmykov, B. A. Kniehl, and M. Shaposhnikov, Higgs boson mass and new physics, J. High Energy Phys. 10 (2012) 140; D. Buttazzo, G. Degrassi, P. P. Giardino, G. F. Giudice, F. Sala, A. Salvio, and A. Strumia, Investigating the near-criticality of the Higgs boson, J. High Energy Phys. 12 (2013) 089.

[5] V. Khachatryan *et al.* (CMS Collaboration), Search for a Higgs boson in the mass range from 145 to 1000 GeV decaying to a pair of W or Z bosons, J. High Energy Phys. 10 (2015) 144.

[6] CMS Collaboration, Updated measurements of the Higgs boson at 125 GeV in the two photon decay channel, Report No. CMS-PAS-HIG-13-001.

[7] S. Chatrchyan *et al.* (CMS Collaboration), Measurement of the properties of a Higgs boson in the four-lepton final state, Phys. Rev. D **89**, 092007 (2014).

[8] For an incomplete list, see P. M. Ferreira, R. Santos, H. E. Haber, and J. P. Silva, Mass-degenerate Higgs bosons at 125 GeV in the two-Higgs-doublet model, Phys. Rev. D **87**, 055009 (2013); T. Han, T. Li, S. Su, and L. T. Wang, Nondecoupling MSSM Higgs sector and light superpartners, J. High Energy Phys. 11 (2013) 053; J. Ke, H. Luo, M. x. Luo, K. Wang, L. Wang, and G. Zhu, Revisit to nondecoupling MSSM, Phys. Lett. B **723**, 113 (2013).

[9] M. Carena, S. Gori, I. Low, N. R. Shah, and C. E. M. Wagner, Vacuum stability and Higgs diphoton decays in the MSSM, J. High Energy Phys. 02 (2013) 114.

[10] D. A. Demir and C. S. Ün, Stop on top: SUSY parameter regions, fine-tuning constraints, Phys. Rev. D **90**, 095015 (2014).

[11] I. Gogoladze, F. Nasir, and Q. Shafi, SO(10) as a framework for natural supersymmetry, J. High Energy Phys. 11 (2013) 173.

[12] R. Aaij *et al.* (LHCb Collaboration), First Evidence for the Decay $B_s^0 \to \mu^+\mu^-$, Phys. Rev. Lett. **110**, 021801 (2013).

[13] C. Bobeth, M. Gorbahn, T. Hermann, M. Misiak, E. Stamou, and M. Steinhauser, $B_{s,d} \to l^+l^-$ in the Standard Model with Reduced Theoretical Uncertainty, Phys. Rev. Lett. **112**, 101801 (2014); C. Bobeth, M. Gorbahn, and E. Stamou, Electroweak corrections to $B_{s,d} \to \ell^+\ell^-$, Phys. Rev. D **89**, 034023 (2014); T. Hermann, M. Misiak, and M. Steinhauser, Three-loop QCD corrections to $B_s \to \mu^+\mu^-$, J. High Energy Phys. 12 (2013) 097.

[14] I. Gogoladze, B. He, A. Mustafayev, S. Raza, and Q. Shafi, Effects of neutrino inverse seesaw mechanism on the sparticle spectrum in CMSSM and NUHM2, J. High Energy Phys. 05 (2014) 078.

[15] P. Langacker, The physics of heavy Z' gauge bosons, Rev. Mod. Phys. **81**, 1199 (2009) and references therein.

[16] R. Wendell *et al.* (Super-Kamiokande Collaboration), Atmospheric neutrino oscillation analysis with subleading effects in Super-Kamiokande I, II, and III, Phys. Rev. D **81**, 092004 (2010).

[17] P. Fileviez Perez and S. Spinner, The fate of R parity, Phys. Rev. D **83**, 035004 (2011); V. Barger, P. Fileviez Perez, and S. Spinner, Minimal Gauged U(1)(B-L) Model with Spontaneous R-parity Violation, Phys. Rev. Lett. **102**, 181802 (2009); P. Fileviez Perez and S. Spinner, The minimal theory for R-parity violation at the LHC, J. High Energy Phys. 04 (2012) 118; P. Fileviez Perez and S. Spinner, Supersymmetry at the LHC and the theory of R parity, Phys. Lett. B **728**, 489 (2014).

[18] C. S. Aulakh, A. Melfo, A. Rasin, and G. Senjanovic, Seesaw and supersymmetry or exact R parity, Phys. Lett. B **459**, 557 (1999); P. Fileviez Perez, S. Spinner, and M. K. Trenkel, The LSP stability and new Higgs signals at the LHC, Phys. Rev. D **84**, 095028 (2011); Testing the mechanism for the LSP stability at the LHC, Phys. Lett. B **702**, 260 (2011).

[19] S. Khalil and A. Masiero, Radiative B-L symmetry breaking in supersymmetric models, Phys. Lett. B **665**, 374 (2008).

[20] J. E. Camargo-Molina, B. O'Leary, W. Porod, and F. Staub, The stability of R parity in supersymmetric models extended by U(1)B-L, Phys. Rev. D **88**, 015033 (2013).

[21] S. Khalil and C. S. Un, Muon anomalous magnetic moment in SUSY B-L model with inverse seesaw, arXiv: 1509.05391.

[22] B. Holdom, Two U(1)s and Epsilon charge shifts, Phys. Lett. **166B**, 196 (1986); K. S. Babu, C. F. Kolda, and J. March-Russell, Implications of generalized Z-Z-prime mixing, Phys. Rev. D **57**, 6788 (1998); F. del Aguila, G. D. Coughlan, and M. Quiros, Gauge coupling renormalization with several U(1) factors, Nucl. Phys. **B307**, 633 (1988); **B312**, 751 (1989); F. del Aguila, J. A. Gonzalez, and M. Quiros, Renormalization group analysis of extended electroweak models from the heterotic string, Nucl. Phys. **B307**, 571 (1988); R. Foot and X. G. He, Comment on Z Z-prime mixing in extended gauge theories, Phys. Lett. B **267**, 509 (1991); T. Matsuoka and D. Suematsu, Low-energy gauge interactions from the $E(8)$ X $E(8)$-prime superstring theory, Prog. Theor. Phys. **76**, 901 (1986); M. E. Krauss, B. O'Leary, W. Porod, and F. Staub, Implications of gauge kinetic mixing on Z' and slepton production at the LHC, Phys. Rev. D **86**, 055017 (2012); R. M. Fonseca, M. Malinsky, W. Porod, and F. Staub, Running soft parameters in SUSY models with multiple U(1) gauge factors, Nucl. Phys. **B854**, 28 (2012).

[23] B. O'Leary, W. Porod, and F. Staub, Mass spectrum of the minimal SUSY B-L model, J. High Energy Phys. 05 (2012) 042.

[24] P. H. Chankowski, S. Pokorski, and J. Wagner, Z-prime and the Appelquist-Carrazzone decoupling, Eur. Phys. J. C **47**, 187 (2006); M. Abbas and S. Khalil, Neutrino masses, mixing and leptogenesis in TeV scale B—L extension of the standard model, J. High Energy Phys. 04 (2008) 056.

[25] M. Abbas and S. Khalil, Neutrino masses, mixing and leptogenesis in TeV scale B—L extension of the standard model, J. High Energy Phys. 04 (2008) 056; L. Basso, The Higgs sector of the minimal SUSY $B-L$ model, Adv. High Energy Phys. **2015**, 1 (2015).

[26] R. N. Mohapatra and J. W. F. Valle, Neutrino mass and baryon number nonconservation in superstring models, Phys. Rev. D **34**, 1642 (1986); M. C. Gonzalez-Garcia and J. W. F. Valle, Fast decaying neutrinos and observable flavor violation in a new class of Majoron models, Phys. Lett. B **216**, 360 (1989); S. Khalil, TeV-scale gauged B-L symmetry with inverse seesaw mechanism, Phys. Rev. D **82**, 077702 (2010); M. Hirsch, M. Malinsky, W. Porod, L. Reichert, and F. Staub, Hefty MSSM-like light Higgs in extended gauge models, J. High Energy Phys. 02 (2012) 084; M. Hirsch, W. Porod, L. Reichert, and F. Staub, Phenomenology of the minimal supersymmetric $U(1)_{B-L} \times U(1)_R$ extension of the standard model, Phys. Rev. D **86**, 093018 (2012).

[27] A. Elsayed, S. Khalil, and S. Moretti, Higgs mass corrections in the SUSY B-L model with inverse seesaw, Phys. Lett. B **715**, 208 (2012); S. Khalil, TeV-scale gauged B-L symmetry with inverse seesaw mechanism, Phys. Rev. D **82**, 077702 (2010).

[28] W. Porod, SPheno, a program for calculating supersymmetric spectra, SUSY particle decays and SUSY particle production at e+ e- colliders, Comput. Phys. Commun. **153**, 275 (2003); W. Porod and F. Staub, SPheno 3.1: extensions including flavor, CP phases and models beyond the MSSM, Comput. Phys. Commun. **183**, 2458 (2012).

[29] F. Staub, Sarah, arXiv:0806.0538; Automatic calculation of supersymmetric renormalization group equations and self energies, Comput. Phys. Commun. **182**, 808 (2011).

[30] J. Hisano, H. Murayama, and T. Yanagida, Nucleon decay in the minimal supersymmetric SU(5) grand unification, Nucl. Phys. **B402**, 46 (1993); Y. Yamada, SUSY and GUT threshold effects in SUSY SU(5) models, Z. Phys. C **60**, 83 (1993); J. L. Chkareuli and I. G. Gogoladze, Unification picture in minimal supersymmetric SU(5) model with string remnants, Phys. Rev. D **58**, 055011 (1998).

[31] L. E. Ibanez and G. G. Ross, $SU(2)_L \times U(1)$ symmetry breaking as a radiative effect of supersymmetry breaking in GUTs, Phys. Lett. **110B**, 215 (1982); K. Inoue, A. Kakuto, H. Komatsu, and S. Takeshita, Aspects of grand unified models with softly broken supersymmetry, Prog. Theor. Phys. **68**, 927 (1982); **70**, 330 (1983); L. E. Ibanez, Locally supersymmetric SU(5) grand unification, Phys. Lett. **118B**, 73 (1982); J. R. Ellis, D. V. Nanopoulos, and K. Tamvakis, Grand unification in simple supergravity, Phys. Lett. **121B**, 123 (1983); L. Alvarez-Gaume, J. Polchinski, and M. B. Wise, Minimal low-energy supergravity, Nucl. Phys. **B221**, 495 (1983).

[32] T. E. W. Group (CDF and D0 Collaborations), Combination of CDF and D0 results on the mass of the top quark, Reprt No. FERMILAB-TM-2427-E.

[33] I. Gogoladze, R. Khalid, S. Raza, and Q. Shafi, Higgs and sparticle spectroscopy with gauge-Yukawa unification, J. High Energy Phys. 06 (2011) 117.

[34] I. Gogoladze, Q. Shafi, and C. S. Un, Higgs boson mass from t-b-τ Yukawa unification, J. High Energy Phys. 08 (2012) 028; M. Adeel Ajaib, I. Gogoladze, Q. Shafi, and C. S. Un, A predictive Yukawa unified SO(10) model: Higgs and sparticle Masses, J. High Energy Phys. 07 (2013) 139.

[35] G. Belanger, F. Boudjema, A. Pukhov, and R. K. Singh, Constraining the MSSM with universal gaugino masses and implication for searches at the LHC, J. High Energy Phys. 11 (2009) 026; H. Baer, S. Kraml, S. Sekmen, and H. Summy, Dark matter allowed scenarios for Yukawa-unified SO(10) SUSY GUTs, J. High Energy Phys. 03 (2008) 056.

[36] K. A. Olive *et al.* (Particle Data Group Collaboration), Review of particle physics, Chin. Phys. C **38**, 090001 (2014).

[37] Y. Amhis *et al.* (Heavy Flavor Averaging Group Collaboration), Averages of B-Hadron, C-Hadron, and tau-lepton properties as of early 2012, arXiv:1207.1158.

[38] D. Asner *et al.* (Heavy Flavor Averaging Group Collaboration), Averages of b-hadron, c-hadron, and $\tau-$lepton properties, arXiv:1010.1589.

[39] The ATLAS Collaboration, Search for pair-production of gluinos decaying via stop and sbottom in events with b-jets and large missing transverse momentum in $\sqrt{s} = 13$ TeV pp collisions with the ATLAS detector, Report No. ATLAS-CONF-2015-067.

[40] See for instance H. Baer, I. Gogoladze, A. Mustafayev, S. Raza, and Q. Shafi, Sparticle mass spectra from SU(5) SUSY GUT models with $b-\tau$ Yukawa coupling unification, J. High Energy Phys. 03 (2012) 047; T. Li, D. V. Nanopoulos, S. Raza, and X. C. Wang, A realistic intersecting D6-brane model after the first LHC run, J. High Energy Phys. 08 (2014) 128; L. Basso, B. O'Leary, W. Porod, and F. Staub, Dark matter scenarios in the minimal SUSY B-L model, J. High Energy Phys. 09 (2012) 054.

[41] M. Davier, A. Hoecker, B. Malaescu, and Z. Zhang, Reevaluation of the hadronic contributions to the muon g-2 and to alpha(MZ), Eur. Phys. J. C **71**, 1 (2011); M. Davier, A. Hoecker, B. Malaescu, and Z. Zhang, Eur. Phys. J. C **72**, 1874 (2012); K. Hagiwara, R. Liao, A. D. Martin, D. Nomura, and T. Teubner, (g-2)mu and alpha(MZ2) reevaluated using new precise data, J. Phys. G **38**, 085003 (2011).

[42] G. W. Bennett *et al.* (Muon g-2 Collaboration), Final report of the muon E821 anomalous magnetic moment measurement at BNL, Phys. Rev. D **73**, 072003 (2006); An improved limit on the muon electric dipole moment, Phys. Rev. D **80**, 052008 (2009).

[43] T. Moroi, The muon anomalous magnetic dipole moment in the minimal supersymmetric standard model, Phys. Rev. D **53**, 6565 (1996); **56**, 4424 (1997); S. P. Martin and J. D. Wells, Muon anomalous magnetic dipole moment in supersymmetric theories, Phys. Rev. D **64**, 035003 (2001); G. F. Giudice, P. Paradisi, A. Strumia, and A. Strumia, Correlation between the Higgs decay rate to two photons and the muon g—2, J. High Energy Phys. 10 (2012) 186.

[44] M. A. Ajaib, I. Gogoladze, Q. Shafi, and C. S. Ün, Split sfermion families, Yukawa unification and muon $g-2$,

J. High Energy Phys. 05 (2014) 079; I. Gogoladze, F. Nasir, Q. Shafi, and C. S. Un, Nonuniversal gaugino masses and muon g-2, Phys. Rev. D **90**, 035008 (2014); K. S. Babu, I. Gogoladze, Q. Shafi, and C. S. Ün, Muon g-2, 125 GeV Higgs boson, and neutralino dark matter in a flavor symmetry-based MSSM, Phys. Rev. D **90**, 116002 (2014); B. P. Padley, K. Sinha, and K. Wang, Natural supersymmetry, muon $g-2$, and the last crevices for the top squark, Phys. Rev. D **92**, 055025 (2015).

[45] M. Flanz, E. A. Paschos, and U. Sarkar, Baryogenesis from a lepton asymmetric universe, Phys. Lett. B **345**, 248 (1995); **382**, 447 (1996); M. Flanz, E. A. Paschos, U. Sarkar, and J. Weiss, Baryogenesis through mixing of heavy Majorana neutrinos, Phys. Lett. B **389**, 693 (1996); L. Covi, E. Roulet, and F. Vissani, *CP*-violating decays in leptogenesis scenarios, Phys. Lett. B **384**, 169 (1996); A. Pilaftsis, *CP* violation and baryogenesis due to heavy Majorana neutrinos, Phys. Rev. D **56**, 5431 (1997).

[46] Y. Grossman, T. Kashti, Y. Nir, and E. Roulet, Leptogenesis from Supersymmetry Breaking, Phys. Rev. Lett. **91**, 251801 (2003); E. J. Chun, Late leptogenesis from radiative soft terms, Phys. Rev. D **69**, 117303 (2004); Y. Grossman, T. Kashti, Y. Nir, and E. Roulet, New ways to soft leptogenesis, J. High Energy Phys. 11 (2004) 080; Y. Grossman, R. Kitano, and H. Murayama, Natural soft leptogenesis, J. High Energy Phys. 06 (2005) 058; Y. Kajiyama, S. Khalil, and M. Raidal, Electron EDM and soft leptogenesis in supersymmetric B-L extension of the standard model, Nucl. Phys. **B820**, 75 (2009).

[47] L. Calibbi, A. Mariotti, C. Petersson, and D. Redigolo, Selectron NLSP in gauge mediation, J. High Energy Phys. 09 (2014) 133; I. Gogoladze, Q. Shafi, and C. S. Ün, Reconciling the muon g2, a 125 GeV Higgs boson, and dark matter in gauge mediation models, Phys. Rev. D **92**, 115014 (2015).

[48] A. Djouadi, The anatomy of electroweak symmetry breaking. I: The Higgs boson in the standard model, Phys. Rep. **457**, 1 (2008).

[49] A. Djouadi, The anatomy of electroweak symmetry breaking. II. The Higgs bosons in the minimal supersymmetric model, Phys. Rep. **459**, 1 (2008).